Jpn. J. Appl. Phys. Vol. 33 (1994) pp. 4782–4786
Part 1, No. 8, August 1994

Characteristics of Hall Accelerator with He, H_2, CH_4, O_2 and Ar Gases

Morihiro OKADA[1], Hisayuki TOKU, Yasushi YAMAMOTO and Kiyoshi YOSHIKAWA
Institute of Atomic Energy, Kyoto University, Uji, Kyoto 611
[1]*Advanced Materials & Technology Research Laboratories, Nippon Steel Corporation, Nakahara-ku, Kawasaki 211*

(Received February 9, 1994; accepted for publication June 18, 1994)

Discharge characteristics and extracted ion beam energy distributions of a Hall-accelerator-type ion source for low-voltage continuous operation (HALOC) with He, H_2, CH_4, Ar and O_2 gases have been studied, and discussed in terms of gas species, electron scattering cross section (total cross section) of ions, electron mean free time, cycloidal length, and the neutralization of ions in the extracted beam.

KEYWORDS: Hall accelerator, electron, cyclotron frequency, mean free time, total scattering cross section, ion beam, energy distribution, magnetron discharge, glow discharge, helium, hydrogen, methane, oxygen, argon

1. Introduction

A Hall accelerator[1)] has a simple configuration and no exhaustible filament so it is easy to generate beams with large current and large cross section of even reactive species such as oxygen ions. A Hall accelerator is a unique ion source for film deposition and surface arrangements, because the energy distribution of extracted ions is broad, and this characteristic seems to be unfavorable for applications to material science. For this reason, the primary applications of a Hall accelerator remain in the fields of space propulsion and fusion reactors.[1,2)] A Hall-accelerator-type ion source for low-voltage continuous operation (HALOC) was designed to produce ions of less than 1 keV. The HALOC has successfully formed hard (4500 kgf/mm^2 Vickers hardness) and adhesive (21 kgf/mm^2 adhesion by scratch test) diamondlike carbon films on iron using methane gas.[3)] It is assumed that ion beams with broad energy distributions are effective in depositing hard and adhesive diamondlike carbon, but details of energy profiles of extracted ion beams had not been determined. Therefore, the relationships between helium ion beam energy distributions and operation parameters of the HALOC were studied by us.[4)] In this research, using He, H_2, CH_4, Ar and O_2 gases, comparisons of discharge characteristics and ion beam energy profiles are studied. The energy distributions of ion beams were observed by a multigrid analyzer.

2. Experimental

The schematic of the HALOC and the electric circuit for beam production are shown in ref. 4. Ion beams are observed using a multigrid analyzer and details of these experimental instruments are described in ref. 4.

3. Discharge Characteristics of Five Kinds of Gases

Figure 1 shows discharge characteristics of five different kinds of gases over a wide range of pressures with 1.0 A discharge current. This figure shows that the discharge voltage for He gas is strongly influenced by the magnetic field at low pressures. In contrast, the discharge voltage for Ar and O_2 gases are less influenced by the magnetic field. In the HALOC, magnetron discharge or glow discharge can occur. In the case of magnetron discharge, when

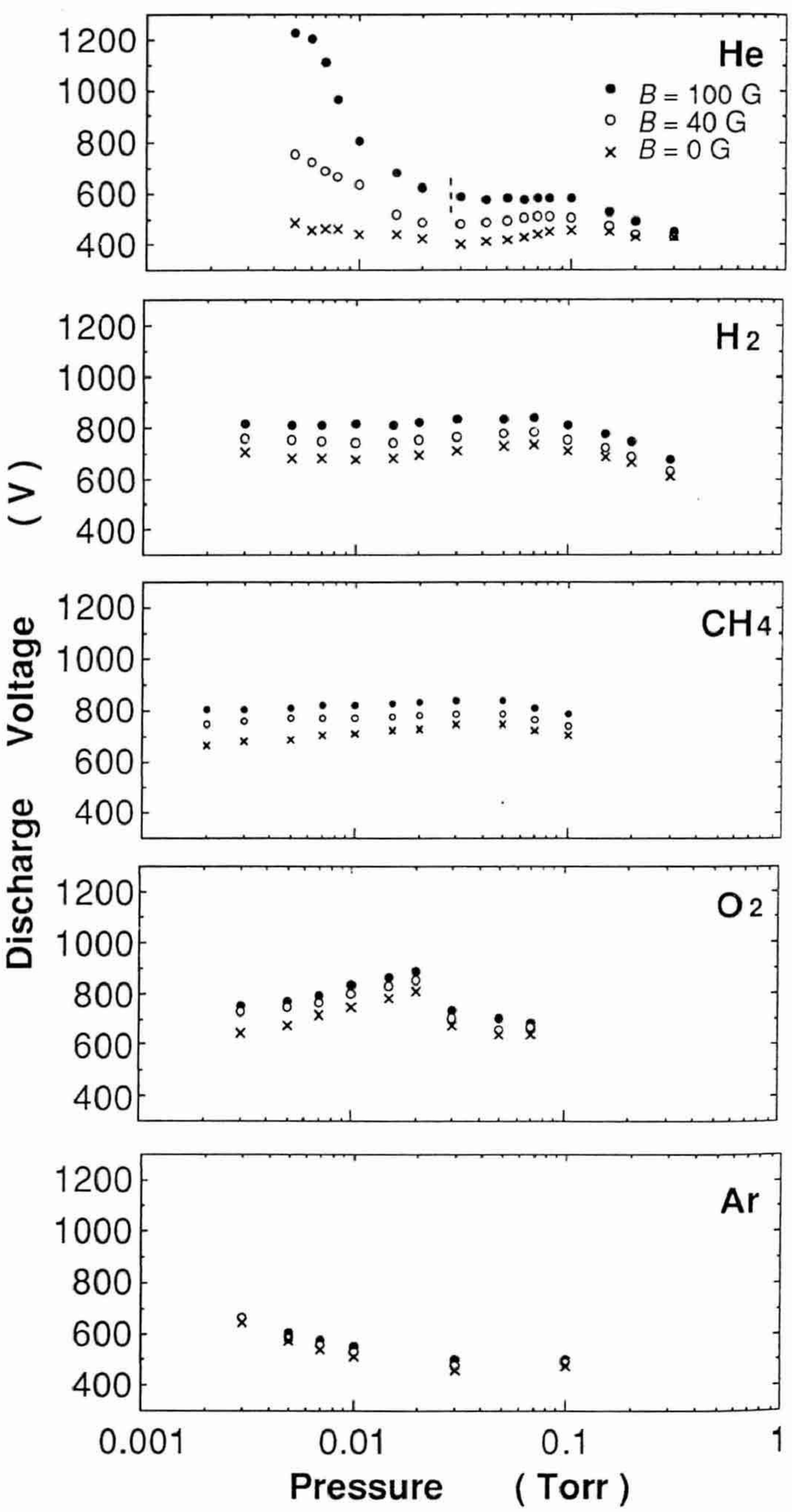

Fig. 1. Discharge characteristics of He, H_2, CH_4, O_2 and Ar over a wide range of pressures with 1.0 A discharge current. ● 1.0×10^{-2} T (100 G) magnetic field in the HALOC, ○ 4.0×10^{-3} T (40 G), × no magnetic field. The dashed line is at the pressure where $\omega\tau=27.6$ (ω: the cyclotron frequency of electrons, τ: the mean free time of electrons) is satisfied under the 1.0×10^{-2} T magnetic field in the He discharge.

Table I. Data of electrons and gas interactions.

	First ionization potential[a]	Total scattering cross section of electron σ_e in gas ($\times 10^{-16}$ cm^2)					Total ionization cross section by electron impact ($\times 10^{-17}$ cm^2)			
	(eV)	10 eV	20 eV	25 eV	50 eV	100 eV	20 eV	40 eV	50 eV	100 eV
He	24.59	4.40	3.01	2.61	1.70	1.09	0	1.7	2.4	3.7
H_2	15.43	10.4	6.5	5.5	3.7	2.52	3.0	8.6	9.5	9.2
CH_4	12.51	25.5	19.4	17.3	12.1	9.0	12	34	38	42
O_2	12.07	10.0	9.4	9.3	9.2	7.7	3.1	16	21	27
Ar	15.76	18.5	21.9	19.0	11.1	8.2	7.4	25	28	30

[a]From ref. 5.

$$\omega\tau \gg 1 \tag{1}$$

is satisfied (ω: the cyclotron frequency of electrons in the discharge channel in the HALOC, τ: the mean free time of electrons in gas), the electron can undergo the cycloidal orbit substantially, and can survive longer in the discharge channel to maintain the magnetron discharge.[4] Under this condition, conduction current j_c in the discharge channel is influenced by the magnetic field as

$$j_c \propto \frac{E^2}{B^2}, \tag{2}$$

where E is the electric field and B is the magnetic flux density in the discharge channel. Characteristic of magnetron discharge is the observation of ions with broad energy distribution.[4]

On the other hand, in the case where

$$\omega\tau \leq 1, \tag{3}$$

electrons collide frequently with gas species before completion of cycloidal motion, and consequently, the magnetic field has relatively little influence on the discharge voltage. Total scattering cross sections of an electron in the gases are shown in Table I. The cross section values of electrons in He, H_2, O_2 and Ar gases are taken from ref. 6. The values for methane gas are taken from ref. 7. The cyclotron frequency of electrons ω and the mean free time of electrons τ are expressed as

$$\omega = \frac{eB}{m_e} \tag{4}$$

$$\tau = \frac{1}{n\sigma_e v} = \frac{1}{n\sigma_e}\sqrt{\frac{m_e}{2W_e}}, \tag{5}$$

where e: electron charge, m_e: electron mass, B: radial magnetic flux density in the discharge channel (80 mm from the exit) and 40 mm radially from the axis of the HALOC, n: gas density, σ_e: total scattering cross section of an electron in gas, v: electron velocity and W_e: electron kinetic energy. On the other hand, the electric fields extend into the chamber through the cathodes, and cathode-glow discharge occurs. Under the condition of $\omega\tau \leq 1$, ion beams generated preferentially by the glow discharge are observed.

Figure 2 shows electron mean free time τ in each gas. τ is calculated according to eq. (5) on the assumption that electron energy is 50 eV. When the hydrogen discharge was actually measured, the electric field in the HALOC was not uniform and electron energy exceeded 45 eV in the vicinity of the anode.[8] The electron energies in the discharge of other gases were not observed. In this paper, the electron energy of 50 eV is considered to be representative in the discharge of the five kinds of gases.

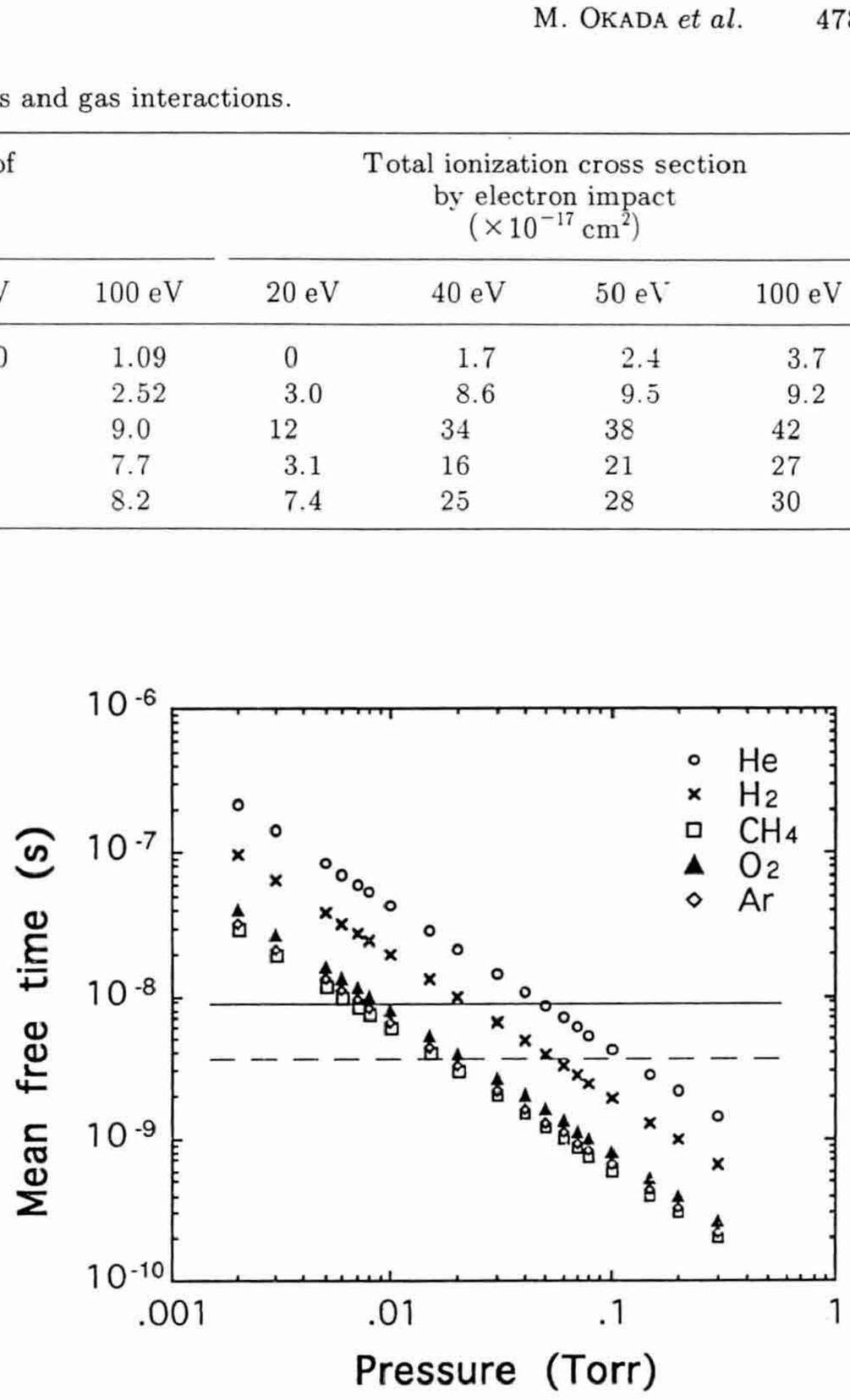

Fig. 2. Mean free time τ of an electron with energy of 50 eV in five kinds of gases under various pressures. The periods of electrons in the cyclotron orbit under 1.0×10^{-2} T and 4.0×10^{-3} T magnetic fields are shown with the solid line (——) and dashed line (– – –), respectively.

3.1 *Discharge of He*

The $\omega\tau$ value of He gas is estimated at first from the point of view of whether the magnetron discharge is predominant or not. With increasing pressure, the electron mean free time decreases as an inverse function and magnetron discharge is not observed in the higher pressure region. According to ref. 4 and Fig. 1, the maximum pressure at which magnetron discharge of He is observed is $P=2\times10^{-2}$ Torr for $B=100\times10^{-4}$ T, and $P=1\times10^{-2}$ Torr for $B=40\times10^{-4}$ T. The values of $\omega\tau$ at the critical pressures where ions generated by magnetron discharge of He appear or disappear are shown in Table II. The values of τ (mean free time)

Table II. $\omega\tau$ value at the critical pressures where ions generated by magnetron discharge appear or disappear in the discharge of He.

Magnetic field (T)	Electron energy (eV)	Maximum pressure at which magnetron discharge is observed		Minimum pressure at which magnetron discharge is not observed	
		Pressure	$\omega\tau$	Pressure	$\omega\tau$
40×10^{-4}	25	1.0×10^{-2} Torr	27.6	1.5×10^{-2} Torr	18.4
	50		30.0		20.0
	100		33.0		22.0
100×10^{-4}	25	2.0×10^{-2} Torr	34.5	3.0×10^{-2} Torr	23.0
	50		37.4		25.0
	100		41.3		27.5

are taken from Fig. 2. Table II indicates that when

$$\omega\tau \geq 27.6, \tag{6}$$

magnetron discharge is observed and when

$$\omega\tau < 27.6, \tag{7}$$

magnetron discharge is not observed and only glow discharge is observed in the discharge of He in the HALOC.[4] The dashed line shown in He discharge in Fig. 1 marks at the critical pressure where $\omega\tau=27.6$ under the 1.0×10^{-2} T magnetic field.

3.2 *Discharge of Ar and He*

The comparison of helium and argon discharges is discussed, because of their simple ion species in practically single-ionized states. An electron's total scattering cross section in Ar gas is larger than that in He gas, and the value $\omega\tau$ of Ar discharge is smaller than that of He gas under the same pressure and the same magnetic field. From the point of view of the value $\omega\tau$, the Ar pressure of 3×10^{-3} Torr ($\tau=2.17\times10^{-8}$ s) corresponds to the He pressure of 2×10^{-2} Torr ($\tau=2.13\times10^{-7}$ s) according to Fig. 2. However, Fig. 1 shows that at 3×10^{-3} Torr of Ar pressure, the discharge is less affected by the magnetic field than the discharge at the He pressure of 2×10^{-2} Torr. According to Table I, the first ionization potential of Ar is lower than that of He and the total ionization cross sections of Ar are larger than those of He; consequently, more Ar gas is ionized by the cathode glow discharge, because there is a substantial extension of electric fields around the cathodes.[9] This is why discharge of Ar is less influenced by the magnetic field and shows weaker magnetron discharge characteristics.

3.3 *Discharge of five kinds of gases*

Figure 1 shows that, in the order of He, H_2, CH_4, O_2 to Ar, discharge voltage is decreasingly influenced by the magnetic field and the pressure. This order corresponds to the total scattering cross section of electrons σ_e in these gases, since, in the above order, the value σ_e increases, the mean free time of electrons τ decreases, and electrons collide more frequently with gases before completion of the cycloidal motion, as mentioned after eq. (3). The values of the total scattering cross section of an electron σ_e (Table I) is in this order except CH_4.

For CH_4, the total scattering cross sections of an electron σ_e are equal to or somewhat bigger than those for Ar, so it is expected that discharge of CH_4 is nominally influenced by the magnetic field similarly to Ar discharge. However, in practice, CH_4 shows discharge characteristics similar to H_2. This may be because CH_4 generates hydrogen species in the discharge.

4. Ion Beam Energy Distributions

Figure 3 shows ion beam energy distribution profiles of the five kinds of gases observed by the multigrid analyzer (MGA) which was placed 250 mm below the beam exit, and 40 mm radially from the center axis of the HALOC. The broad lines between the profiles are at the pressures where $\omega\tau=27.6$ was satisfied (see §3.1). The HALOC was operated over a range of pressures with 1.0 A discharge current and 1.0×10^{-2} T magnetic field, and the discharge voltages are shown in Fig. 1. The MGA at 0 rad faces the HALOC and detects not only the ion beams coming straight from the HALOC, but also the low-energy ions generated and accelerated by the sheath around the MGA.[4] The MGA at $\pi/2$ rad is, on the other hand, at a right angle to the HALOC and only detects the ions due to the sheath around the MGA. In order to distinguish between the ions from the HALOC and the ions due to the sheath around the MGA, the ion beam energy distributions are observed with the MGA at 0 rad and also with the MGA at $\pi/2$ rad with respect to the HALOC. The hatched parts in Fig. 3 are energy profiles of ions originating from magnetron discharge in the HALOC.

In discussing the ion beam energy distribution profiles in Fig. 3, the following two factors are considered. One is discharge type (glow and magnetron) in the HALOC, and the other is the ratio of detected ions originating from the HALOC to those due to the sheath around the MGA.

For the He ion beam energy profile at 2×10^{-2} Torr, ions with a broad energy distribution around 300–500 eV (hatched part) are assumed to originate from magnetron discharge in the HALOC, but at 3×10^{-2} Torr, few of those ions are observed because the critical pressure where the magnetron discharge of He appears or disappears is between 2×10^{-2} Torr and 3×10^{-2} Torr (see §3.1). At 3×10^{-3} Torr, the discharge of He was ob-

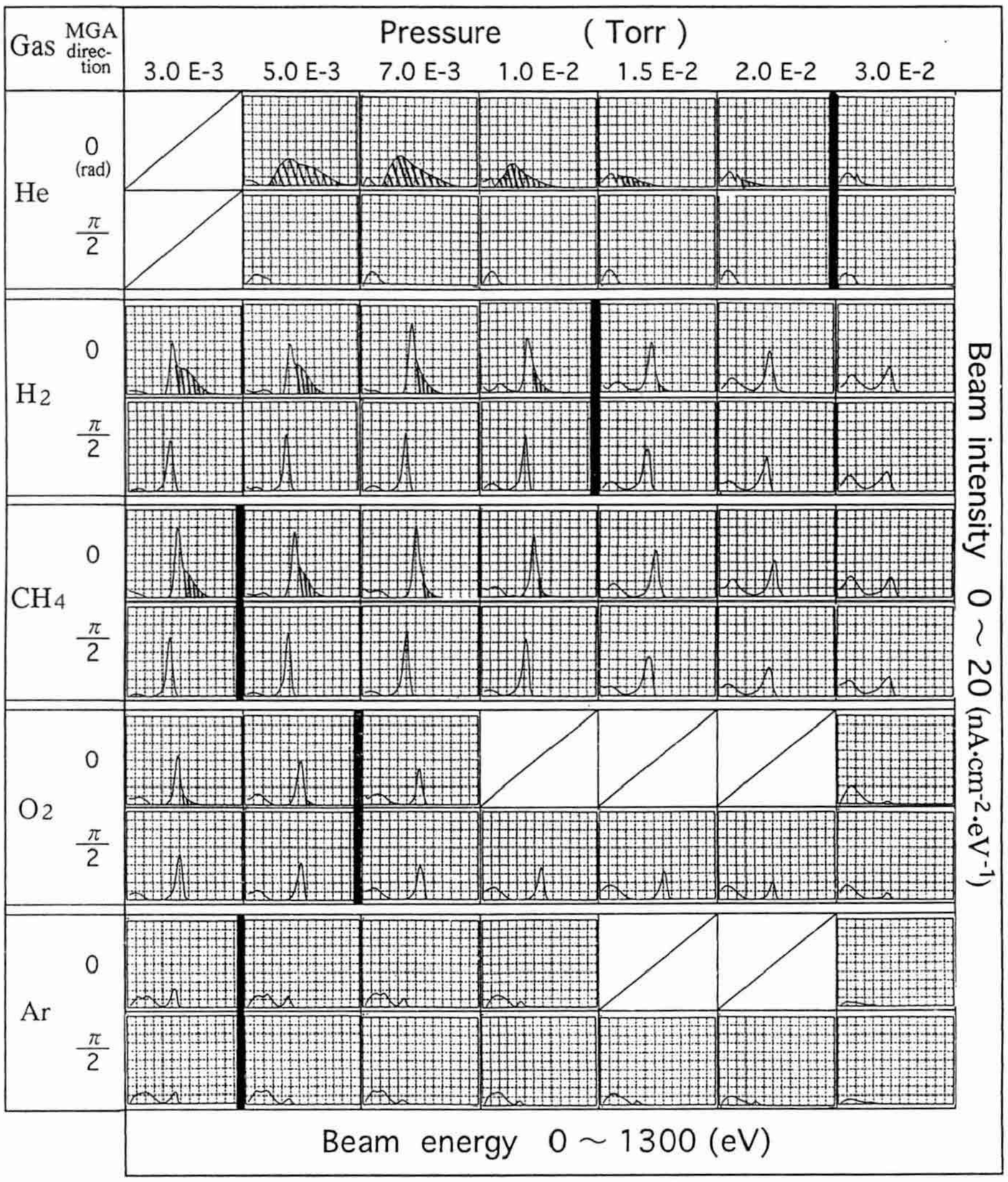

Fig. 3. Ion beam energy distribution profiles of five kinds of gases observed by the MGA placed 250 mm below the beam exit and 40 mm radially from the center axis of the HALOC. The HALOC was operated with 1.0 A discharge current and 1.0×10^{-2} T magnetic field. The broad lines between the profiles are at the pressures where $\omega\tau=27.6$ was satisfied. The hatched areas of the energy profiles are of ions originating from magnetron discharge in the HALOC.

served to be unstable and subject to breakdown.

In the energy profile of H_2, ions with broad energy distribution due to the magnetron discharge (hatched part) are observed in the range from 3×10^{-3} Torr to 1×10^{-2} Torr. With increase of the pressure, the number of those ions decrease, and at pressures equal to or higher than 1.5×10^{-2} Torr, very few ions with broad energy distribution from the HALOC are observed. This pressure corresponds to the critical pressure (1.2×10^{-2} Torr for $\omega\tau=27.6$) of H_2 discharge.

For CH_4, the critical pressure is found to be around 3.8×10^{-3} Torr ($\omega\tau=27.6$). but the ion beam energy profiles of CH_4 show broad energy distributions due to the magnetron discharge at higher pressures, and the profiles and intensities of the beams are similar to those of H_2. This may be because CH_4 generates hydrogen species in the discharge. It is not yet known, however, how many hydrogen ions are contained in these ion beams.

For O_2, few ions are observed due to the magnetron discharge in the pressure lower than the critical pressure (5.0×10^{-3} Torr for $\omega\tau=27.6$). At higher pressures, on the other hand, energy profiles observed at 0 rad and at $\pi/2$ rad do not show appreciable differences. In the observation of O_2, when the MGA faced the HALOC, arclike discharges occurred among the electrodes in the MGA during the measurements under pressures from 1.0×10^{-2} Torr to 2.0×10^{-2} Torr, so ions from the HALOC could not be observed.

At pressures lower than the critical pressure, a considerable number of ions from the HALOC are observed in the discharge of He and H_2. However, in the discharge of Ar, very few ions originating from the HALOC are observed because the size of Ar (0.38 nmϕ Van der Waals diameter) is larger than that of He (0.30 nmϕ) or H (0.24 nmϕ), so the scattering cross section of Ar ions in Ar gas is assumed to be larger than those of He ions and H ions in their respective gases. Consequently, more Ar ions are scattered enroute (250 mm) from the exit of the HALOC to the MGA, and thus cannot be detected. For a He ion beam, the number of ions arriving at MGA without scattering and neutralization was calculated.[4] However, this number could not be calculated for other gases due to the in-

sufficient amounts of a data for cross section of scattering and charge exchange reported.

Observed energy profiles of ion beams generated by the HALOC are influenced by the following four factors: (a) ion species, (b) discharge type (magnetron or cathode glow) in the HALOC, (c) interactions between ion beam and atmospheric gas in the chamber, and (d) drifting ions accelerated by the sheath around the MGA. For a He ion beam, ion species are simple, and fast ion and gas interaction data are available in sufficient amounts (discussed in detailed in ref. 4), and the relationships between the discharge types and ion beam energy profiles are rather simple and clear. From this point of view, the concept of the critical pressure where $\omega\tau=27.6$ is satisfied is given. It is assumed that the value at which $\omega\tau=27.6$ will be affected by the structural parameters (length and volume of the discharge channel and strength of E and B) of the HALOC. For H_2, CH_4 and O_2, ion species are complex, and in the cases of O_2 and Ar, ion beams are strongly influenced by the atmospheric gas. Consequently, the concept of the critical pressure does not always seem to apply to the analysis of energy profiles of these gases. However, if the condition $\omega\tau=27.6$ is applied to each species (in the cases of CH_4 discharge, CH_x, C, H, $H_2, \cdots$, for example) according to their quantities, the relationships between discharge conditions and beam energy profiles will be clarified, and we believe that the critical pressure may be an effective concept in order to design an effective Hall accelerator which can generate ion beams with intended energy profiles. Further study is necessary to prove these hypotheses.

5. Conclusions

The following is concluded in this study.

1. Using He, H_2, CH_4, O_2, and Ar gas, the HALOC was successfully operated.

2. For He, H_2 and O_2, under low pressures where $\omega\tau \geq 27.6$ (ω: the cyclotron frequency of electrons in the HALOC, τ: the mean free time of electrons in gas) was satisfied, ions which originated from magnetron discharge in the HALOC exhibit broad energy distributions. Under high pressures where $\omega\tau<27.6$ was satisfied, ions from the magnetron discharge are not predominantly observed.

3. CH_4 shows discharge characteristics and ion beam energy profiles similar to those of H_2. This may be due to the fact that the discharge of CH_4 produces ion species similar to those in H_2 discharge.

4. At 25 cm from the HALOC, almost all the Ar ions detected by the MGA originate from the sheath around the MGA even under the lowest (3×10^{-3} Torr) pressure, since Ar ions originating in the HALOC are mostly scattered enroute (25 cm) to the MGA and thus, cannot be detected.

1) A. I. Morozov, Yu. V. Esinchuk, G. N. Tilinin, A. V. Trofimov, Yu. A. Sharov and G. Ya. Shchepkin: Sov. Phys. Tech. Phys. **17** (1972) 38.
2) E. A. Pinsley and C. O. Brown: J. Spacecraft & Rockets **1** (1964) 525.
3) M. Okada, H. Toku, Y. Yamamoto and K. Yoshikawa: Jpn. J. Appl. Phys. **31** (1992) 1845.
4) M. Okada, H. Toku, Y. Yamamoto and K. Yoshikawa: Jpn. J. Appl. Phys. **32** (1993) 4826.
5) *CRC Handbook of Chemistry and Physics*, ed. D. R. Lide (Chemical Rubber Company, Florida, 1992) 73rd ed.
6) M. Hayashi: *Recommended Values of Transport Cross Sections for Elastic Collision and Total Collision Cross Section for Electrons in Atomic and Molecular Gases* (Nagoya Institute of Technology, Nagoya, 1981) IPPJ-AM-19.
7) International Atomic Energy Agency: *Atomic and Plasma-Material Interaction Data for Fusion* (International Atomic Energy Agency, Vienna, 1992) Vol. 2, p. 41.
8) H. Iinuma, K. Nakada, H. Toku, Y. Yamamoto and K. Yoshikawa: Bull. Inst. At. Energy Kyoto Univ. **76** (1989) 37 [in Japanese].
9) H. Iinuma, K. Nakada, H. Toku, Y. Yamamoto and K. Yoshikawa: Bull. Inst. At. Energy Kyoto Univ. **75** (1989) 36 [in Japanese].